Talanta 129 (2014) 411–416

Contents lists available at ScienceDirect

Talanta

journal homepage: www.elsevier.com/locate/talanta

Facile fabrication of an ultrasensitive sandwich-type electrochemical immunosensor for the quantitative detection of alpha fetoprotein using multifunctional mesoporous silica as platform and label for signal amplification

Yulan Wang [a], Xiaojian Li [a], Wei Cao [a], Yueyun Li [b], He Li [a], Bin Du [a], Qin Wei [a,*]

[a] Key Laboratory of Chemical Sensing & Analysis in Universities of Shandong, School of Chemistry and Chemical Engineering, University of Jinan, Jinan 250022, PR China
[b] School of Chemical Engineering, Shandong University of Technology, Zibo 255049, PR China

ARTICLE INFO

Article history:
Received 4 March 2014
Received in revised form
9 June 2014
Accepted 10 June 2014
Available online 17 June 2014

Keywords:
Sandwich-type electrochemical immunosensor
Alpha fetoprotein
MCM-41
Toluidine blue
Gold nanoparticles

ABSTRACT

A novel and ultrasensitive sandwich-type electrochemical immunosensor was designed for the quantitative detection of alpha fetoprotein (AFP) using multifunctional mesoporous silica (MCM-41) as platform and label for signal amplification. MCM-41 has high specific surface area, high pore volume, large density of surface silanol groups (Si–OH) and good biocompatibility. MCM-41 functionalized with 3-aminopropyltriethoxysilane (APTES), gold nanoparticles (Au NPs) and toluidine blue (TB) could enhance electrochemical signals. Moreover, primary antibodies (Ab_1) and secondary antibodies (Ab_2) could be effectively immobilized onto the multifunctional MCM-41 by the interaction between Au NPs and amino groups ($-NH_2$) on antibodies. Using multifunctional MCM-41 as a platform and label could greatly simplify the fabrication process and result in a high sensitivity of the designed immunosensor. Under optimal conditions, the designed immunosensor exhibited a wide liner range from 10^{-4} ng/mL to 10^3 ng/mL with a low detection limit of 0.05 pg/mL for AFP. The designed immunosensor showed acceptable selectivity, reproducibility and stability, which could provide potential applications in clinical monitoring of AFP.

1. Introduction

As a member of the albuminoid gene family, alpha fetoprotein (AFP) is a tumor-associated fetal protein produced by the fetal liver and yolk sac [1]. The expressional level of AFP is highly elevated in hepatocellular carcinoma [2], which is one of the most common malignancies in the world, generally followed by liver cirrhosis or chronic infection with hepatitis B or C virus [3]. Therefore, AFP has been considered as one of the most important tumor markers in diagnosing and targeting of hepatocellular carcinoma [4]. In addition, AFP may function as a direct or indirect factor associated with hepatoma growth [5].

In recent years, a number of methods were proposed for the quantitative detection of AFP in human serum, such as latex particle immunoassay [6], supplementation counterimmunoelectrophoresis [7], time-resolved fluorometry [8], electrochromatography [9], radioimmunoassay [10], chemiluminescent sandwich enzyme immunoassays [11] and enzyme-linked immunosorbent assay [12]. Compared with these methods, electrochemical immunoassays with fast analysis, low detection limit, high sensitivity and simple instrumentation have recently attracted extensive attention and have been extensively applied in the detection of tumor markers [13,14].

In order to improve the sensitivity of the electrochemical immunoassays, all kinds of mesoporous materials have been used for signal amplification in construction of electrochemical immunosensors [15,16]. Mesoporous silica (MCM-41) has many advantages including highly ordered hexagonal pores, high specific surface area, tunable pore diameter, high pore volume, large density of surface silanol groups (Si–OH) and good biocompatibility [17]. Moreover, MCM-41 has demonstrated functional applications as solid supports to anchor variety of guest compounds like metal nanoparticles and dyes [18]. All these advantages mentioned above could be beneficial to the effective immobilization of antibodies and redox probes in electrochemical immunoassays. Therefore, MCM-41 has potential applications in the fabrication of electrochemical immunosensors.

* Corresponding author. Tel.: +86 531 82765730; fax: +86 531 82765969.
E-mail address: sdjndxwq@163.com (Q. Wei).

http://dx.doi.org/10.1016/j.talanta.2014.06.017
0039-9140/

In this work, an ultrasensitive sandwich-type electrochemical immunosensor was designed for the quantitative detection the AFP in human serum. MCM-41 functionalized with 3-aminopropyltriethoxysilane (APTES), gold nanoparticles (Au NPs) and toluidine blue (TB) was used as a platform and label for signal amplification in this strategy. TB was used to provide the electrochemical signal of the designed immunosensor as a kind of electron transfer mediators containing amino groups ($-NH_2$). Au NPs were decorated on the surface or in the pore of MCM-41 to increase the load of TB by the interaction between Au NPs and $-NH_2$ on TB. Moreover, primary antibodies (Ab_1) and secondary antibodies (Ab_2) could be effectively immobilized onto the multifunctional MCM-41 (Au@MCM-41/TB/Ab_1 and Au@MCM-41/TB/Ab_2) by the interaction between Au NPs and $-NH_2$ on antibodies. Therefore, using multifunctional MCM-41 as a platform and label could greatly simplify the fabrication process and enhance the sensitivity of the designed sandwich-type electrochemical immunosensor.

2. Materials and methods

2.1. Apparatus and reagents

All electrochemical measurements were performed on a CHI760D electrochemical workstation (Chenhua Instrument Shanghai Co., Ltd., China). Transmission electron microscope (TEM) images were obtained from a Hitachi H-600 microscope (Japan). Scanning electron microscope (SEM) images were obtained using Quanta FEG250 field emission environmental SEM (FEI, United States) operated at 4 KV. UV–vis measurements were carried out using a Lambda 35 UV/vis Spectrometer (Perkin-Elmer, United States). Surface area measurements were performed on Micromeritics ASAP 2020 surface area and porosity analyzer (Quantachrome, United States).

Human AFP antigen and antibody to human AFP were purchased from Shanghai Linc-Bio Science Co., Ltd., China. MCM-41 was purchased from Nanjing XF NANO Co., Ltd., China. APTES was purchased from Shanghai Aladdin Chemistry Co., Ltd., China. TB was purchased from Sinopharm Chemical Reagent Co., Ltd., China. Phosphate buffered saline (PBS) was used as an electrolyte for all electrochemistry measurements. All other reagents were of analytical grade and ultrapure water was used throughout the study.

2.2. Preparation of the amino-functionalized MCM-41

Amino-functionalized MCM-41 (NH_2-MCM-41) was synthesized following the procedure reported previously with some modification [19]. Briefly, MCM-41 (0.5 g) was dispersed in 20 mL of anhydrous toluene with 0.5 mL of APTES and heated to 70 °C under stirring for 1.5 h, then centrifuged and dried at 110 °C. After the reaction of APTES and Si–OH on MCM-41, a free-flowing powdery material was obtained. The NH_2-MCM-41 was shown to contain $-NH_2$ by the ninhydrin test [20].

2.3. Preparation of the gold nanoparticles decorated MCM-41

Gold nanoparticles decorated MCM-41 (Au@MCM-41) was prepared by a simple method. Briefly, 0.8 mL of 1 wt% $HAuCl_4$ was added dropwise into 100 mL of aqueous solution containing 5 mg of $NaBH_4$ under stirring in ice bath. A ruby-red uniformly dispersed solution containing Au NPs in an approximate concentration of 0.2 mM was obtained. 20 mL of ultrapure water containing 20 mg of NH_2-MCM-41 was under continuous ultrasound for 1 h to disperse uniformly, which was added into 100 mL of prepared Au NPs solution under stirring. The Au@MCM-41 was obtained by the interaction between Au NPs and $-NH_2$ on MCM-41 after mild centrifugation and dried in vacuum at 35 °C.

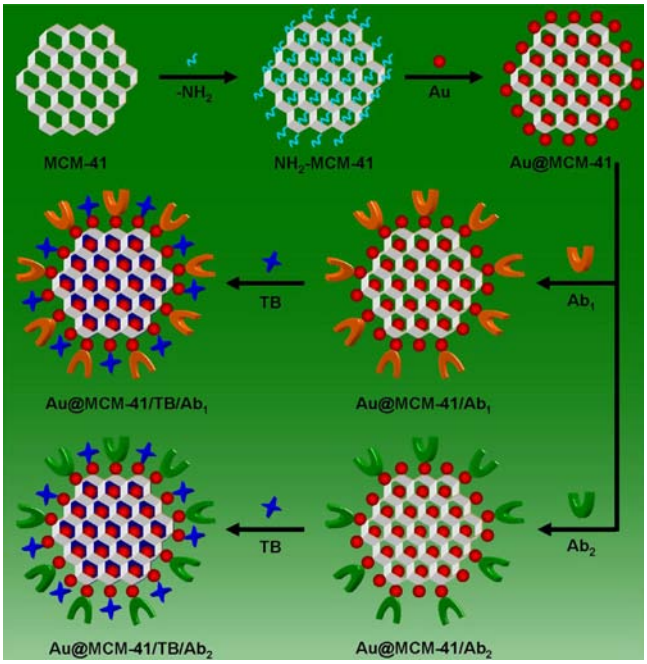

Fig. 1. The preparation procedures of Au@MCM-41/TB/Ab_1 and Au@MCM-41/TB/Ab_2.

2.4. Preparation of the Au@MCM-41/TB/Ab_1 and Au@MCM-41/TB/Ab_2

Fig. 1 shows the preparation procedures of Au@MCM-41/TB/Ab_1 and Au@MCM-41/TB/Ab_2. In brief, Au@MCM-41 (1 mg/mL, 1 mL) was added into the solution of Ab_1 (10 μg/mL, 1 mL) and Ab_2 (10 μg/mL, 1 mL) and stirred for 12 h at 4 °C. After centrifugation, a solution of TB (2 mg/mL, 1 mL) was added into the obtained precipitate (Au@MCM-41/Ab_1 and Au@MCM-41/Ab_2), and stirred for another 12 h at 4 °C. Following centrifugation, the resulting Au@MCM-41/TB/Ab_1 and Au@MCM-41/TB/Ab_2 were dispersed in 0.5 mL of PBS at pH 7.4 and stored at 4 °C.

2.5. Fabrication of the immunosensor

Fig. 2 shows the schematic diagram of the designed sandwich-type electrochemical immunosensor. A glassy carbon electrode (GCE) with 4 mm diameter was polished to a mirror-like finish with 1.0, 0.3 and 0.05 mm alumina powder successively and then thoroughly washed with ultrapure water before use. First, 6 μL of Au@MCM-41/TB/Ab_1 solution was added onto the electrode and dried at 4 °C. After washing, 3 μL of 1 wt% bovine serum albumin (BSA) solution was added and incubated for 1 h to eliminate nonspecific binding sites. Following that, the electrode was washed and incubated with a varying concentration of AFP for 1 h at room temperature, and then the electrode was washed extensively to remove unbounded AFP molecules. Finally, 6 μL of Au@MCM-41/TB/Ab_2 solution was added onto the electrode surface for another 1 h at room temperature, the electrode was washed thoroughly and ready for measurement.

2.6. Detection of AFP

A conventional three-electrode system was used for all electrochemical measurements: a GCE as the working electrode, a

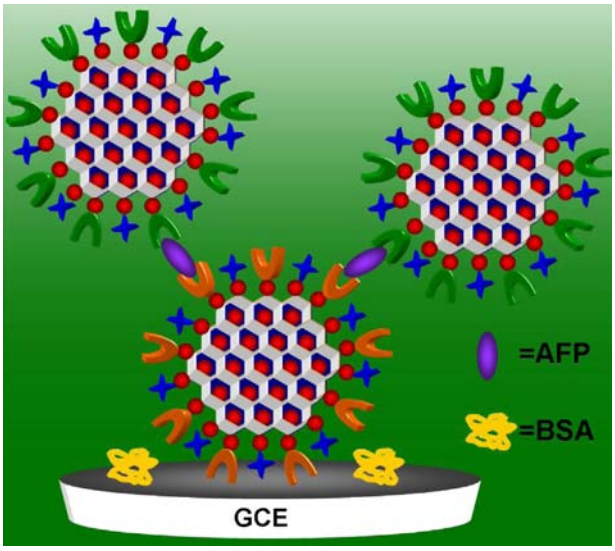

Fig. 2. The schematic diagram of the immunosensor.

saturated calomel electrode (SCE) as the reference electrode, and a platinum wire electrode as the counter electrode. The PBS at pH 6.8 was used for all the electrochemical measurements. Differential pulse voltammetry (DPV) and cyclic voltammograms (CVs) were recorded in PBS by scanning the potential from −0.6 V to 0.2 V.

3. Results and discussion

3.1. Characterization of the MCM-41, NH_2-MCM-41 and Au@MCM-41

Fig. 3A shows the SEM image of the MCM-41 with a size of approximate 2 μm. The TEM image (Fig. 3B) of the MCM-41 confirmed that it possessed the ordered silica channels. The MCM-41 had a BET surface area of 935 m^2/g (Fig. 3D) and an average BJH pore size of 3.5 nm (Fig. 3E). Due to the high pore volume and large specific surface area, a large number of Au NPs could be decorated successfully in the pore of NH_2-MCM-41 and on the surface of it (Fig. 3C). The UV–vis spectrums (Fig. 3F) were used to further confirm that Au NPs could be successfully connected on NH_2-MCM-41. Pure Au NPs solution had a major peak at 507 nm (curve *a*). No absorption peak was observed for the NH_2-MCM-41 (curve *b*). When Au NPs was connected with the NH_2-MCM-41, an absorption peak around 507 nm was also observed (curve *c*), indicating the successful synthesis of Au@MCM-41 [21].

3.2. Optimization of experimental conditions

In order to achieve an optimal electrochemical signal, the optimization of experimental conditions including pH and the concentration of Au@MCM-41 was necessary. The optimal DPV oxidation peak current response was achieved at pH 6.8 (Fig. 4A) and 2.0 mg/mL of Au@MCM-41 (Fig. 4B). Under the optimal conditions, the designed immunosensor could exhibit an optimal electrochemical signal for the quantitative detection of AFP.

3.3. Characterization of the immunosensor

DPV was used to verify that TB could produce the electrochemical signal of the designed immunosensor (Fig. 5A). It could be observed that the bare GCE modified with TB exhibited an obvious oxidation peak at −0.26 V (curve *c*). When Au@MCM-41/TB/Ab_1 (curve *a*) was modified on bare GCE, an oxidation peak at −0.26 V could also be observed attributing to TB connected with Au@MCM-41. When Au@MCM-41/TB/Ab_2/AFP/BSA/Au@MCM-41/TB/Ab_1 (curve *b*) was modified on the electrode, an increasing oxidation peak could be observed at −0.24 V. The right shift of oxidation peak might be due to the modification of the biological active substance.

In order to characterize the fabrication process of the immunosensor, CVs at each modification step were recorded in PBS at pH 6.8 (Fig. 5B). First, Au@MCM-41/TB/Ab_1 (curve *b*) was modified on a bare GCE (curve *a*) and generated an obvious redox peak due to the presence of TB. and then BSA (curve *c*) and AFP (curve *d*) were modified on the electrode surface, the redox peak current was declined because of biological active substances that hindered the efficiency of electron transfer. Finally, when Au@MCM-41/TB/Ab_2 (curve *e*) was modified on the electrode surface, an obvious increasing redox peak was observed due to the increasing number of TB.

The A.C. impedance method was also used to characterize the fabrication process of the sandwich-type electrochemical immunosensor (Fig. 5C). Nyquist plots of the A.C. impedance methods recorded from 1 to 10^5 Hz at 0.24 V in PBS at pH 7.4 containing 0.1 M KCl and 2.5 mM $Fe(CN)_6^{3-}/Fe(CN)_6^{4-}$. In the Nyquist plots, it is well known that the high frequency region of the impedance plot shows a semicircle related to the redox probe $Fe(CN)_6^{3-}/Fe(CN)_6^{4-}$ and the semicircle diameter is equal to resistance, followed by a Warburg line in the low frequency region which corresponds to the diffusion step of the overall process. It could be observed that the bare GCE exhibited a very small resistance (curve *a*). After modification with Au@MCM-41/TB/Ab_1, a smaller resistance (curve *b*) was observed attributing to the good electron transfer ability of Au@MCM-41. Gradually increasing resistance indicated the successful modification of the non-conductive bioactive substances when BSA (curve *c*) and AFP (curve *d*) were modified layer by layer on the electrode. When Au@MCM-41/TB/Ab_2 (curve *e*) was modified on the electrode, an obvious decrease of resistance could also be observed due to the good electron transfer ability of Au@MCM-41.

Under the optimal conditions, a sandwich-type electrochemical immunosensor based on a simple signal amplification strategy using multifunctional MCM-41 as a platform and label was used to detect different concentrations of AFP. A linear relationship between DPV oxidation peak current responses and the logarithmic values of AFP concentration was obtained covering the concentration range from 10^{-4} ng/mL to 10^3 ng/mL (Fig. 6) and the linear regression equation of the calibration curve was $I = 16.82 + 1.43 \log C$ with correlation coefficient of 0.99. The low detection limit of 0.05 pg/mL was obtained at a signal to noise ratio (S/N) of 3, which was ascribed to the simple signal amplification strategy of the designed sandwich-type electrochemical immunosensor.

3.4. Comparison of different methods

The linear range and detection limit of the designed immunosensor was compared with previously reported methods for the detection of AFP in Table 1. Many research groups have developed different methods [22-36] for the quantitative detection of AFP, some of which [22–24] have achieved detection limits at the level of fg/mL. This designed sandwich-type electrochemical immunosensor in this work has a lower detection and wider detection limit than most of the reported methods for the detection of AFP, specially having a lower detection limit than previously reported sandwich-type electrochemical immunosensors [25–28].

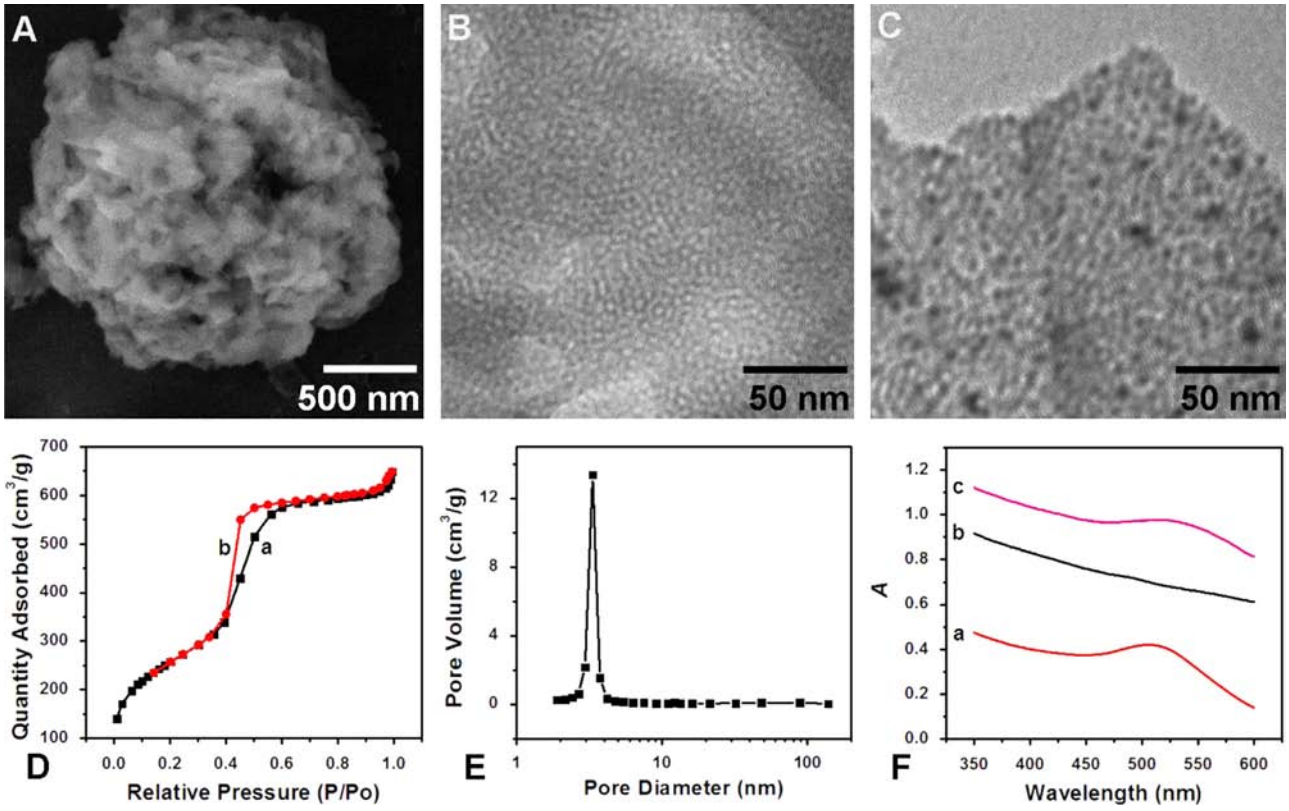

Fig. 3. (A) SEM image of MCM-41; (B) TEM image of MCM-41; (C) TEM image of Au@MCM-41; (D) N_2 adsorption–desorption isotherm of MCM-41; (E) Pore size distribution of MCM-41; and (F) UV–vis spectrums of Au NPs (a), NH_2-MCM-41 (b) and Au@MCM-41 (c).

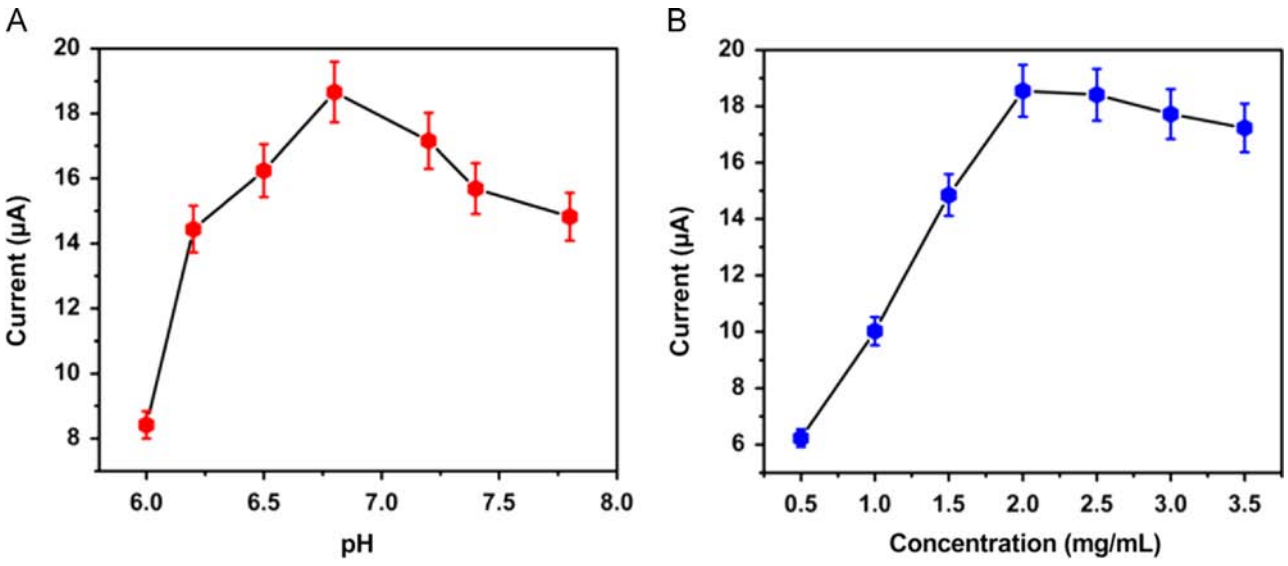

Fig. 4. Effect of pH (A) and the concentration of Au@MCM-41 (B) on the DPV oxidation peak current responses of the immunosensor for the detection of 10 ng/mL of AFP. Error bar = RSD (n = 5).

Consequently, high sensitivity is one of the advantages of this designed immunosensor.

For most sandwich-type immunosensors, the materials of platform were usually different with the materials of label [29], which could increase the complexity of immunosensors. In this work, multifunctional MCM-41 could not only immobilize the antibodies but also produce electrochemical signals. Therefore, multifunctional MCM-41 was used as platform and label simultaneously, which could effectively simplify the process of fabrication of sandwich-type immunosensors. As a result, the facile fabrication procedure is another advantage of this designed immunosensor.

3.5. Reproducibility, selectivity and stability

To evaluate the reproducibility of the immunosensor, a series of five electrodes was prepared for the detection of 100 ng/mL of AFP. DPV was used to record the electrochemical signal in PBS at pH

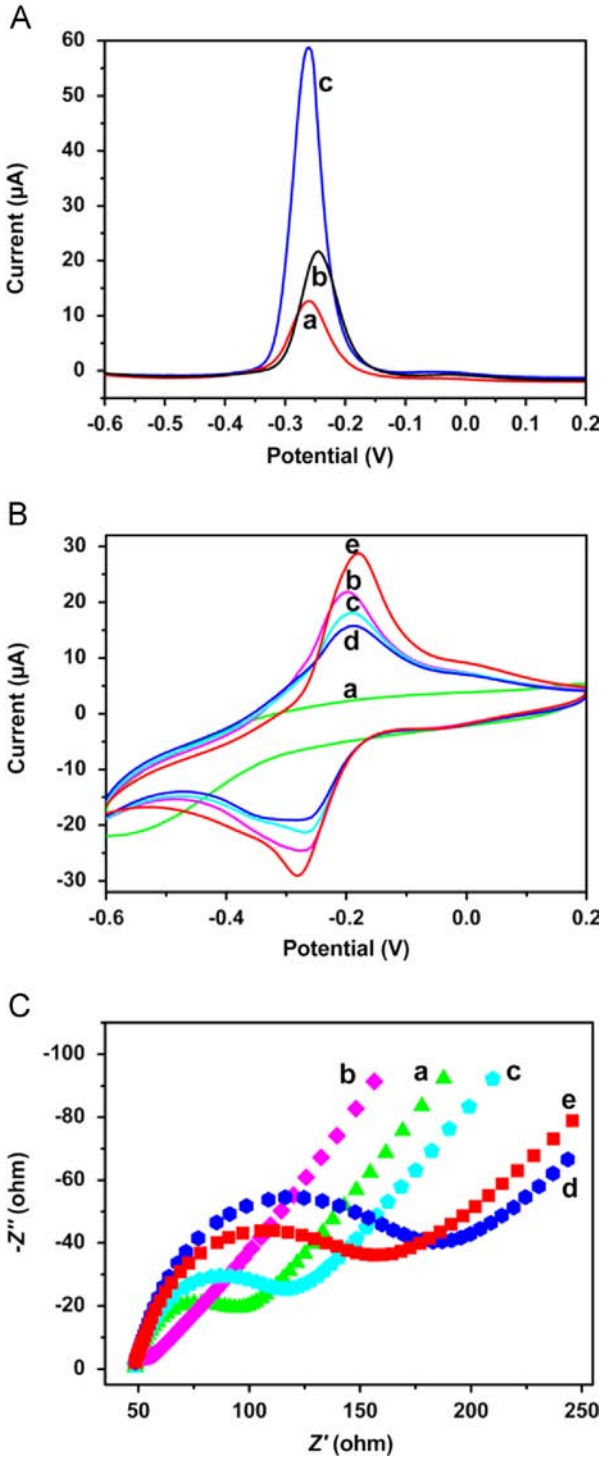

Fig. 5. (A) DPV oxidation peak current responses recorded from −0.6 V to 0.2 V in PBS at pH 6.8: Au@MCM-41/TB/Ab_1/GCE (a), Au@MCM-41/TB/Ab_2/AFP/BSA/Au@MCM-41/TB/Ab_1/GCE (b), TB/GCE (c); (B) CVs recorded from −0.6 V to 0.2 V in PBS at pH 6.8: bare GCE (a), Au@MCM-41/TB/Ab_1/GCE (b), BSA/Au@MCM-41/TB/Ab_1/GCE (c), AFP/BSA/Au@MCM-41/TB/Ab_1/GCE (d) and Au@MCM-41/TB/Ab_2/AFP/BSA/Au@MCM-41/TB/Ab_1/GCE (e); (C) Nyquist plots of the A.C. impedance methods recorded from 1 to 10^5 Hz in PBS at pH 7.4 containing 0.1 M KCl and 2.5 mM Fe$(CN)_6^{3-}$/Fe$(CN)_6^{4-}$: bare GCE (a), Au@MCM-41/TB/Ab_1/GCE (b), BSA/Au@MCM-41/TB/Ab_1/GCE (c), AFP/BSA/Au@MCM-41/TB/Ab_1/GCE (d) and Au@MCM-41/TB/Ab_2/AFP/BSA/Au@MCM-41/TB/Ab_1/GCE (e).

6.8 by scanning the potential from −0.6 V to 0.2 V and the concentration of Au@MCM-41 is 2.0 mg/mL. The relative standard deviation (RSD) of the measurements for the five electrodes was

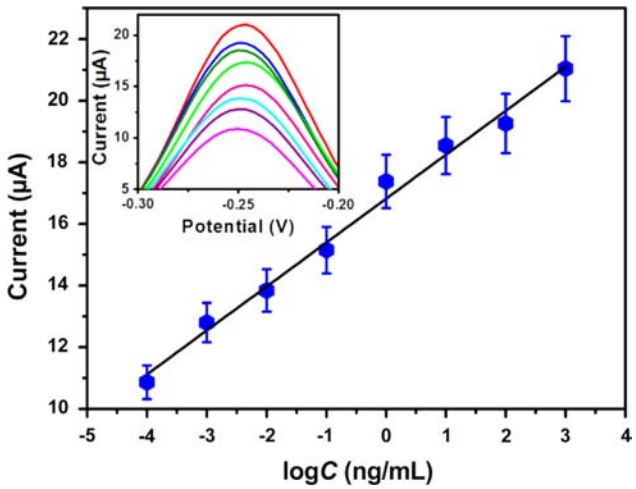

Fig. 6. Calibration curve of the immunosensor towards different concentrations of AFP. Error bar=RSD (n=5).

2.06%, suggesting that the precision and reproducibility of the proposed immunosensor was quite good.

To investigate the specificity of the fabricated immunosensor, interferences study was performed using carcinoembryonic antigen (CEA), BSA, glucose and vitamin C. The 1 ng/mL of AFP solution containing 100 ng/mL of interfering substances was measured by the designed immunosensor. The current variation due to the interfering substances was less than 5% of that without interferences, indicating that the selectivity of the immunosensor was acceptable.

To test the stability of the immunosensor, the immunosensor for the detection of 100 ng/mL of AFP was stored at 4 °C when not in use. After two weeks, no apparent change was found when compared with the immunosensor which was used to directly detect the same concentration of AFP without being stored. The good stability could be ascribed to the good biocompatibility of Au@MCM-41. The reproducibility, selectivity and stability of this immunosensor was acceptable, thus it was suitable for the determination of AFP in real samples.

3.6. Real sample analysis

In order to test the precision and accuracy of the designed immunosensor, it was used to detect the recoveries of different concentrations of AFP in serum sample by standard addition methods. The results were shown in Table 2 and the RSD between 1.52% and 2.32% were obtained. The recovery was in the range from 99.7% to 101.8%. Thus, the proposed immunosensor could be effectively applied to the determination of AFP in human serum.

4. Conclusions

This work has developed a novel and ultrasensitive sandwich-type immunosensor using multifunctional MCM-41 as a platform and label for signal amplification. The designed immunosensor for the quantitative detection of AFP displayed a linear response with a wide range (10^{-4}∼10^3 ng/mL), a low detection limit (0.05 pg/mL), acceptable reproducibility, selectivity and stability. The facile fabrication procedure plus the ultrasensitivity demonstrated by the designed immunosensor may provide wide potential applications for the detection of AFP in clinical diagnosis.

Table 1
Comparison of different methods for the detection of AFP.

Method	Linear range	Detection limit	Reference
Label-free electrochemiluminescence immunosensor	0.0005–50 pg/mL	0.2 fg/mL	[22]
Sandwich-type electrochemiluminescence immunosensor	0.005–0.2 pg/mL	1.0 fg/mL	[23]
Label-free electrochemical immunosensor	0.00005–250 ng/mL	1.1 fg/mL	[24]
Label-free electrochemical impedance spectroscopy immunosensor	1–100 pg/mL	0.1 pg/mL	[30]
Label-free electrochemical immunosensor	0.001–45 ng/mL	0.13 pg/mL	[31]
Sandwich-type electrochemical immunosensor	0.01–60 ng/mL	1.6 pg/mL	[25]
Label-free electrochemiluminescence immunosensor	0.005–14 ng/mL	2.0 pg/mL	[32]
Sandwich-type electrochemical immunosensor	0.01–40 ng/mL	2.3 pg/mL	[26]
Label-free electrochemical immunosensor	0.01–75 ng/mL	4.0 pg/mL	[13]
Label-free electrochemical immunosensor	0.01–12 ng/mL	5.0 pg/mL	[33]
Sandwich-type electrochemical immunosensor	0.05–30 ng/mL	5.0 pg/mL	[27]
Competitive electrochemical immunosensor	0.05–100 ng/mL	5.0 pg/mL	[34]
Label-free electrochemical immunosensor	0.1–30 ng mL	18 pg/mL	[35]
Sandwich-type electrochemiluminescence immunosensor	0.05–50 ng/mL	30 pg/mL	[36]
Sandwich-type electrochemical immunosensor	0.5–80 ng/mL	250 pg/mL	[28]
Sandwich-type electrochemical immunosensor	0.0001–1000 ng/mL	0.05 pg/mL	This method

Table 2
Determination of AFP in human serum sample.

Initial AFP concentration in sample (ng/mL)	Added AFP concentration (ng/mL)	Measured concentration after addition (ng/mL)	RSD (%, $n=5$)	Recovery (%, $n=5$)
0.97	1.00	1.99, 1.96, 2.05, 1.93, 2.01	2.32	101.8
	5.00	5.91, 6.11, 5.92, 5.95, 5.88	1.52	99.7
	10.00	10.88, 11.19, 10.87, 10.96, 11.27	1.67	100.6

Acknowledgments

This study was supported by the National Natural Science Foundation of China (Nos. 21175057, 21375047 and 21377046), the Science and Technology Plan Project of Jinan (No. 201307010) and QW thanks the Special Foundation for Taishan Scholar Professorship of Shandong Province and UJN (No. ts20130937).

References

[1] Y.-S. Won, S.-W. Lee, J. Biotechnol. 129 (2007) 614–619.
[2] A. Otsuru, S. Nagataki, T. Koji, T. Tamaoki, Cancer 62 (1988) 1105–1112.
[3] J.F. Perz, G.L. Armstrong, L.A. Farrington, Y.J.F. Hutin, B.P. Bell, J. Hepatol. 45 (2006) 529–538.
[4] K. Taketa, Hepatology 12 (1990) 1420–1432.
[5] X.W. Wang, J.H. Yuan, R.G. Zhang, L.X. Guo, Y. Xie, H. Xie, World J. Gastroenterol. 7 (2001) 345–351.
[6] B. Passelecq, M. De, Bo, C. Huber, J.P. Gennart, A. Bernard, R. Lauwerys, J. Immunol. Methods 109 (1988) 69–74.
[7] S.H. Chan, S.H. Heng, M.J. Simons, J. Immunol. Methods 29 (1979) 191–196.
[8] E.P. Diamandis, T.K. Christopoulos, C.C. Bean, J. Immunol. Methods 147 (1992) 251–259.
[9] G.I. Abelev, E.R. Karamova, N.L. Lazarevich, V.I. Kiseleva, A.M. Poverenny, Immunol. Lett. 40 (1994) 133–138.
[10] W. Brummund, D.A. Aryan, M.T. Mennuti, N.A. Starkovsky, Clin. Chim. Acta 105 (1980) 25–40.
[11] S. Aoyagi, M. Kusumi, A. Matsuyuki, M. Maeda, A. Tsuji, J. Immunol. Methods 137 (1991) 73–78.
[12] I.A. Darwish, T.A. Wani, A.M. Alanazi, M.A. Hamidaddin, S. Zargar, Talanta 111 (2013) 13–19.
[13] H. Wang, H. Li, Y. Zhang, Q. Wei, H. Ma, D. Wu, Y. Li, Y. Zhang, B. Du, Biosens. Bioelectron. 53 (2014) 305–309.
[14] F. Yang, J. Han, Y. Zhuo, Z. Yang, Y. Chai, R. Yuan, Biosens. Bioelectron. 55 (2014) 360–365.
[15] Q. Li, D. Tang, J. Tang, B. Su, J. Huang, G. Chen, Talanta 84 (2011) 538–546.
[16] Z. Sun, Z. Luo, C. Gan, S. Fei, Y. Liu, H. Lei, Biosens. Bioelectron. 59 (2014) 99–105.
[17] S.P. Hudson, R.F. Padera, R. Langer, D.S. Kohane, Biomaterials 29 (2008) 4045–4055.
[18] P.R. Selvakannan, K. Mantri, J. Tardio, S.K. Bhargava, J. Colloid Interface Sci. 394 (2013) 475–484.
[19] A. Cauvel, G. Renard, D. Brunel, J. Org. Chem. 62 (1997) 749–751.
[20] P.J. Lamothe, P.G. McCormick, Anal. Chem. 45 (1973) 1906–1911.
[21] Q. Wei, X. Xin, B. Du, D. Wu, Y. Han, Y. Zhao, Y. Cai, R. Li, M. Yang, H. Li, Biosens. Bioelectron. 26 (2010) 723–729.
[22] Z. Guo, T. Hao, J. Duan, S. Wang, D. Wei, Talanta 89 (2012) 27–32.
[23] H. Wang, D. Sun, Z. Tan, W. Gong, L. Wang, Colloids Surf. B. Biointerfaces 84 (2011) 515–519.
[24] K. Liu, J. Zhang, Q. Liu, H. Huang, Electrochim. Acta 114 (2013) 448–454.
[25] Z. Yang, Y. Chai, R. Yuan, Y. Zhuo, Y. Li, J. Han, N. Liao, Sens. Actuators B 193 (2014) 461–466.
[26] G.K. Parshetti, F.-h. Lin, R.-a. Doong, Sens. Actuators B 186 (2013) 34–43.
[27] L. Zhao, S. Li, J. He, G. Tian, Q. Wei, H. Li, Biosens. Bioelectron. 49 (2013) 222–225.
[28] C. Ding, F. Zhao, R. Ren, J.-M. Lin, Talanta 78 (2009) 1148–1154.
[29] Y. Ge, J. Wu, H. Ju, S. Wu, Talanta 120 (2014) 218–223.
[30] H. Yang, Z. Li, X. Wei, R. Huang, H. Qi, Q. Gao, C. Li, C. Zhang, Talanta 111 (2013) 62–68.
[31] B. Kavosi, R. Hallaj, H. Teymourian, A. Salimi, Biosens. Bioelectron. 59 (2014) 389–396.
[32] X. Li, Q. Guo, W. Cao, Y. Li, B. Du, Q. Wei, Anal. Biochem. 457 (2014) 59–64.
[33] T. Qi, J. Liao, Y. Li, J. Peng, W. Li, B. Chu, H. Li, Y. Wei, Z. Qian, Biosens. Bioelectron. 61 (2014) 245–250.
[34] X. Fang, M. Han, G. Lu, W. Tu, Z. Dai, Sens. Actuators B 168 (2012) 271–276.
[35] R.-P. Liang, Z.-X. Wang, L. Zhang, J.-D. Qiu, Sens. Actuators B 166–167 (2012) 569–575.
[36] S. Yuan, R. Yuan, Y. Chai, L. Mao, X. Yang, Y. Yuan, H. Niu, Talanta 82 (2010) 1468–1471.